Supporting Information

Repurposing of tranilast for potential neuropathic pain treatment by inhibition of sepiapterin reductase in the BH_4 pathway

Benjamin J.R. Moore,[1,2] Barira Islam,[1,2] Sean Ward,[3] Olivia Jackson,[3] Rebecca Armitage,[3] Jack Blackburn,[4] Shozeb Haider[5] and Patrick C. McHugh[1,2*]

[1] Centre for Biomarker Research, School of Applied Sciences, University of Huddersfield, Queensgate, Huddersfield, HD1 3DH, UK

[2] Department of Pharmacy, School of Applied Sciences, University of Huddersfield, Queensgate, Huddersfield, HD1 3DH, UK

[3] Innovative Physical Organic Solutions (IPOS), Department of Chemical and Biological Sciences, University of Huddersfield, Queensgate, Huddersfield, HD1 3DH, UK

[4] Department of Chemical Sciences, School of Applied Sciences, University of Huddersfield, Queensgate, Huddersfield, HD1 3DH, UK

[5] UCL School of Pharmacy, 29-39 Brunswick Square, London WC1N 1AX, UK

*To whom the correspondence should be addressed

SUPPORTING TABLES

Table S1. Compounds selected from docking of the LOPAC[1280] library that showed docking scores below -35. The IC_{50} concentrations calculated from *in vitro* SPR protein assays are included, along with their hydrogen bonds formed with the four key binding residues in the starting SPR-sepiapterin complex. The green boxes indicate the presence of a hydrogen bond (bond strength > 1 kcal/mol calculated in Molsoft). The grey boxes indicate no hydrogen bond of the hSPR residue with the drug.

		Interactions With Sepiapterin Binding Residues				
Compound Name	**IC_{50} (µM)**	**S157**	**Y170**	**G199**	**D257**	**Other**
Tranilast	**5.889**					
Nordihydroguaiaretic acid	**8.262**					
N-Acetylserotonin	**11.61**					
Aurintricarboxylic Acid	**33.19**					
6-Chloromelatonin	**37.3**					
Emodin	**62.03**					
N-(4-amino-2-chlorophenyl)pthalimide	**63.46**					
Tyrphostin AG537	**94.63**					
Hispidin	**106.2**					
BIO	**117.9**					
Genistein	**137.2**					
L-732138	**148.8**					
Tyrphostin AG494	**204.3**					
Quercetin Dihydrate	**234.7**					
N-Acetyltryptamine	**246.5**					
Nocodazole	**264.5**					
Supercinnamaldehyde	**362.2**					
Niclosamide	**620.7**					
5,6,7,8-Tetrahydro-L-biopterin	***No Inhibition***					
AS-252424	***No Inhibition***					
Benserazide	***No Inhibition***					
Benzamil	***No Inhibition***					
CP-91149	***No Inhibition***					
Formoterol	***No Inhibition***					
Ofloxacin	***No Inhibition***					
Prazosin	***No Inhibition***					
S(+)- Raclopride L-tartrate	***No Inhibition***					

Table S2. List of antibodies used for western blot studies.

Antibody	Species	Dilution	Supplier	Reference
GCH1	*Hs*	1:500	SantaCruz Biotech	sc-134574
SPR	*Hs*	1:1000	Abcam	ab157194
STAT3	*Hs*	1:1000	ProSci Inc	7197
GAPDH	*Hs*	1:2000	Abcam	ab8245
AlexaFluor 647	*Goat anti-mouse*	1:2000	ThermoFisher LifeTech	A21236
AlexaFluor 546	*Goat anti-rabbit*	1:2000	ThermoFisher LifeTech	A11010

Table S3. List of primer pairs used for qRT-PCR.

Gene	Species	Primer Sequence	Tm(^{o}C)
β-Actin	*Hs*	F: CTTCCAGCCTTCCTTCCTG	60
		R: CTCCTGCTTGCTGATCCAC	60
GAPDH	*Hs*	F: GGTATGGACTGTGGTACTGAG	61.8
		R: TGCACCACCAACTGCTTAGC	59.4
GCH1	*Hs*	F: ACAAACAAAACCGCAACTCC	60
		R: TGGGATGAATTTGAAGAGCA	59
GCHFR	*Hs*	F: TCTGCCTTGCTCCTCTCTTC	60
		R: CCCTCTCCCACTGCTTGAC	61
CTBP1	*Hs*	F: TGTAACTGCTGGACCCAAGG	59.4
		R: TACACGCCTCTGTCATTCGT	59.4
GSK3β	*Hs*	F: CTGTGTGTTGGCTGAGCTGT	59.4
		R: TTTGCTCCCTTGTTGGAGTT	55.3
iNOS	*Hs*	F: CCATAAGGCCAAAGGGATTT	55.3
		R: ATCTGGAGGGGTAGGCTTGT	59.4
SPR	*Hs*	F: GGCTCTCTTGGGGATGTGT	60
		R: TTCAGGACGCTGGAAGTCA	60
STAT1	*Hs*	F: TCAGTCTTTTCCAGCAGCTCA	57.9
		R: CTTCAAGACCAGCGGCCTC	61
STAT3	*Hs*	F: GGGAGAGATTGACCAGCAGTAT	60.3
		R: TGGCTTCTCAAGATACCTGCTC	60.3
NFKB1	*Hs*	F: GAGCAGGCATCCATCGAGAT	59.4
		R: GGCTGTCAGATGGTCCTTGT	57.3
SPHK1	*Hs*	F: ATGCTGGCTATGAGCAGGTC	59.4
		R: GTGCAGAGACAGCAGGTTCA	59.4

SUPPORTING FIGURES

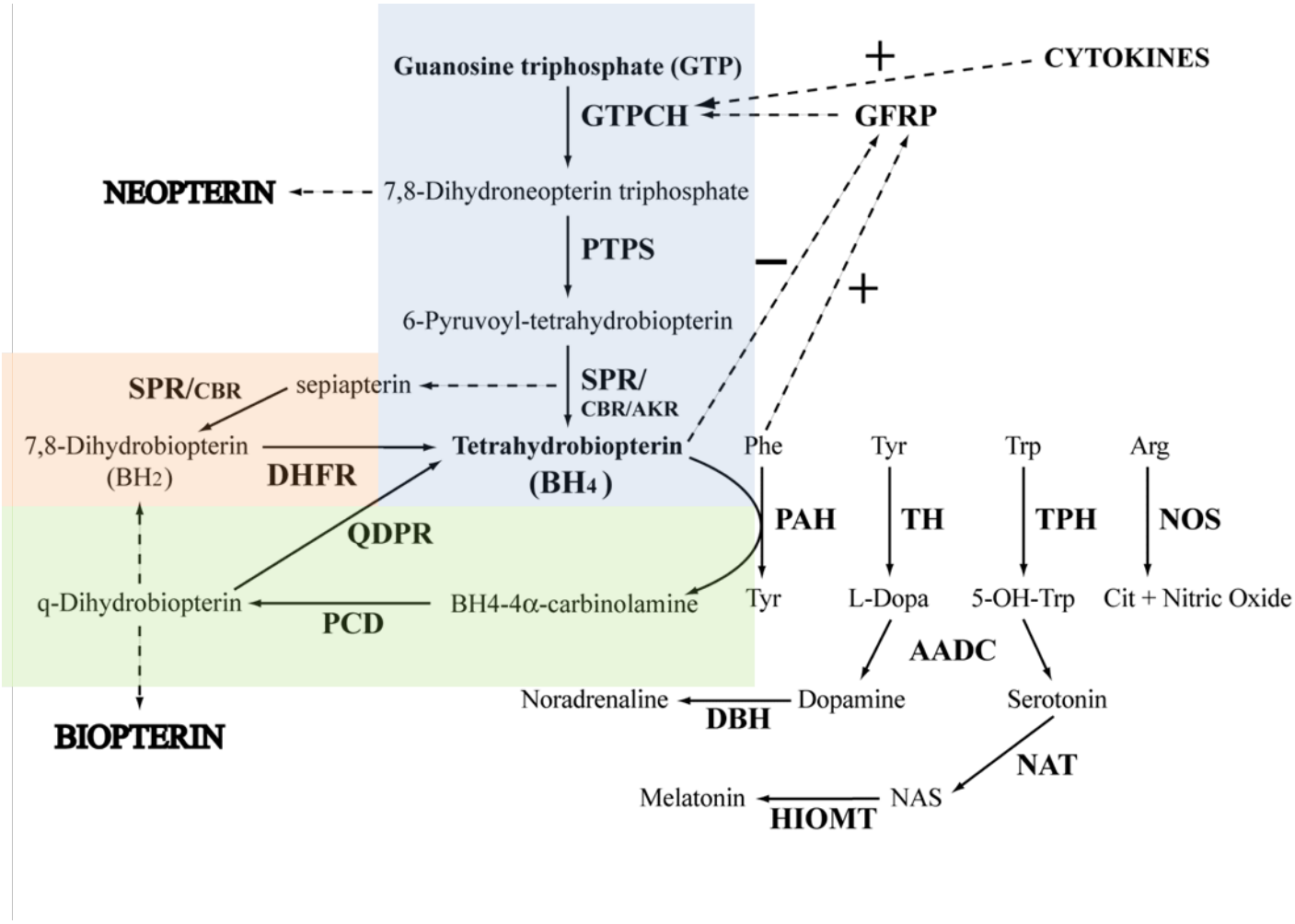

Figure S1. The tetrahydrobiopterin biosynthesis pathways in the body. The *de novo*, salvage and biopterin recycling pathways are shown in blue, orange and green, respectively. The biosynthesis of BH_4 starts *de novo* from guanosine triphosphate (GTP), through reactions catalyzed by the enzymes GTP cyclohydrolase I (GTPCH/GCH1), 6-pyruvoyltetrahydropterin synthase (PTPS) and sepiapterin reductase (SPR). Alternatively, the final two-step reduction of the intermediate 6-pyruvoyl-tetrahydrobiopterin (PPS) to BH_4 can be effected by aldose reductase (AKR) and carbonyl reductase (CBR). The product of both these reactions is sepiapterin, which can be salvaged into BH_4 through SPR, CBR and dihydrofolate reductase (DHFR). Two additional enzymes, pterin-4a-carbinolamine dehydratase (PCD) and dihydropteridine reductase (QDPR) are involved in the regeneration of BH_4 from intermediates formed during the hydroxylation of aromatic amino acids. GCH1 activity is modulated by the interaction of GTP cyclohydrolase feedback regulator (GFRP) and effector molecules, BH_4 and phenylalanine. Phe, phenylalanine; Tyr, tyrosine; Trp, tryptophan; Arg, arginine; Cit, citrulline; PAH, phenylalanine hydroxylase; TH, tyrosine hydroxylase; TPH, tryptophan hydroxylase; NOS, nitric oxide synthase; 5-OH-Trp, 5-hydroxytryptophan; AADC, aromatic amino-acid decarboxylase; DBH, dopamine β-hydroxylase; NAT, N-acetyltransferase; NAS, N-acetylserotonin; HIOMT, hydroxyindole-O-methyltransferase (Figure amended from Reference[33] in the main text).

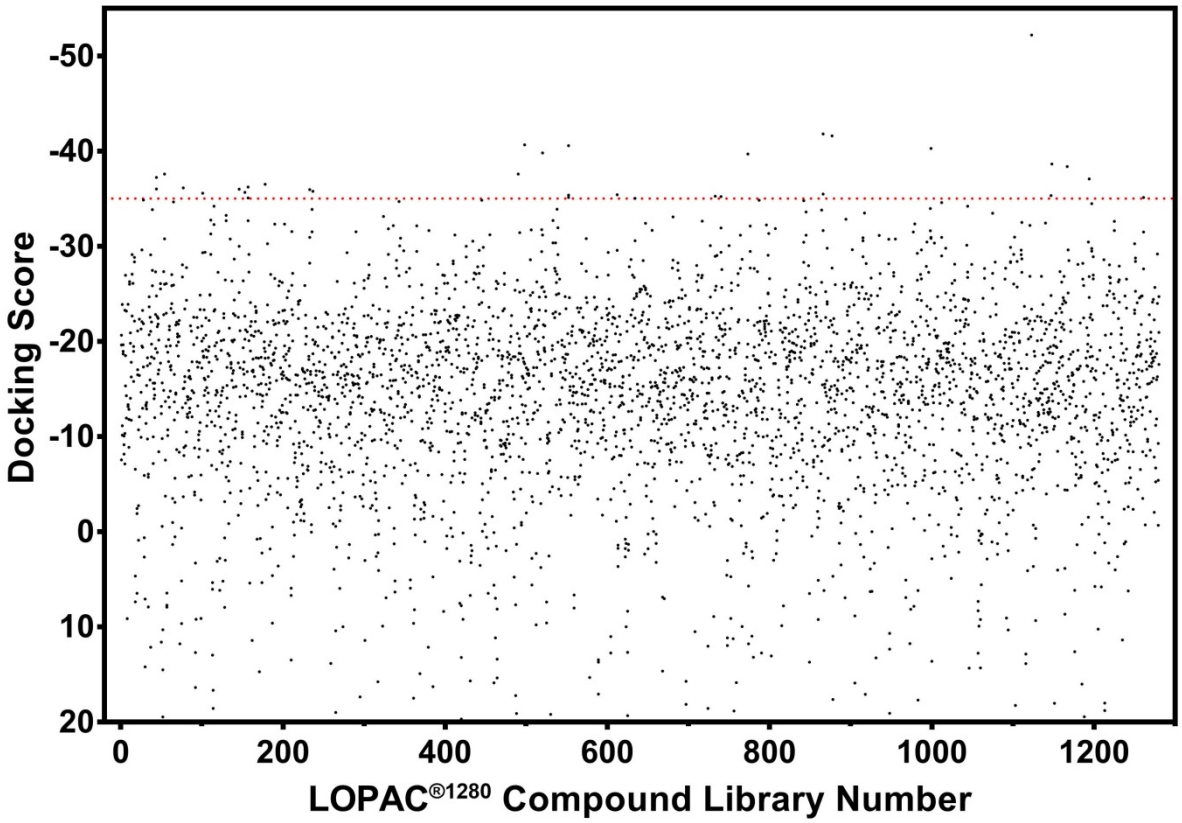

Figure S2. The scores of LOPAC^{1280} compounds on hSPR obtained by using the docking tool of Molsoft ICM. The sepiapterin showed the lowest score of -52.09 (compound number 1123). Only docking scores of 20 and below are shown in the figure. The cut-off of -35 is shown as a red dashed line.

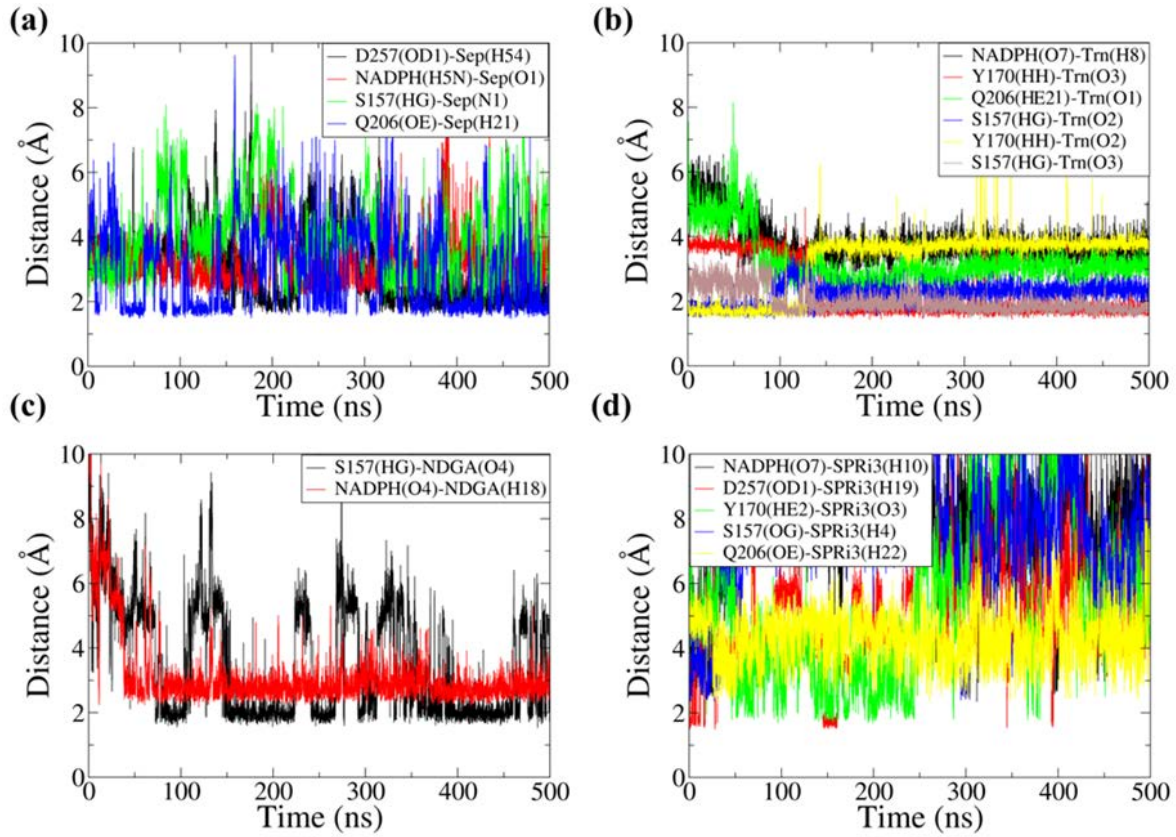

Figure S3. Stability of the hydrogen bonds in the hSPR-drug simulations. The interactions of (a) hSPR-sepiapterin, (b) hSPR-tranilast, (c) hSPR-NDGA and (d) hSPR-SPRi3 are shown in the figure. The aromatic ring of NADPH sampled stacking interactions with aromatic rings of sepiapterin, tranilast and NDGA for some part of the simulations. No stable hydrogen bond was sampled by SPR-SPRi3 complex. A cut-off of 3.5 Å and bond angle of 20˚ was used for hydrogen bond formation.

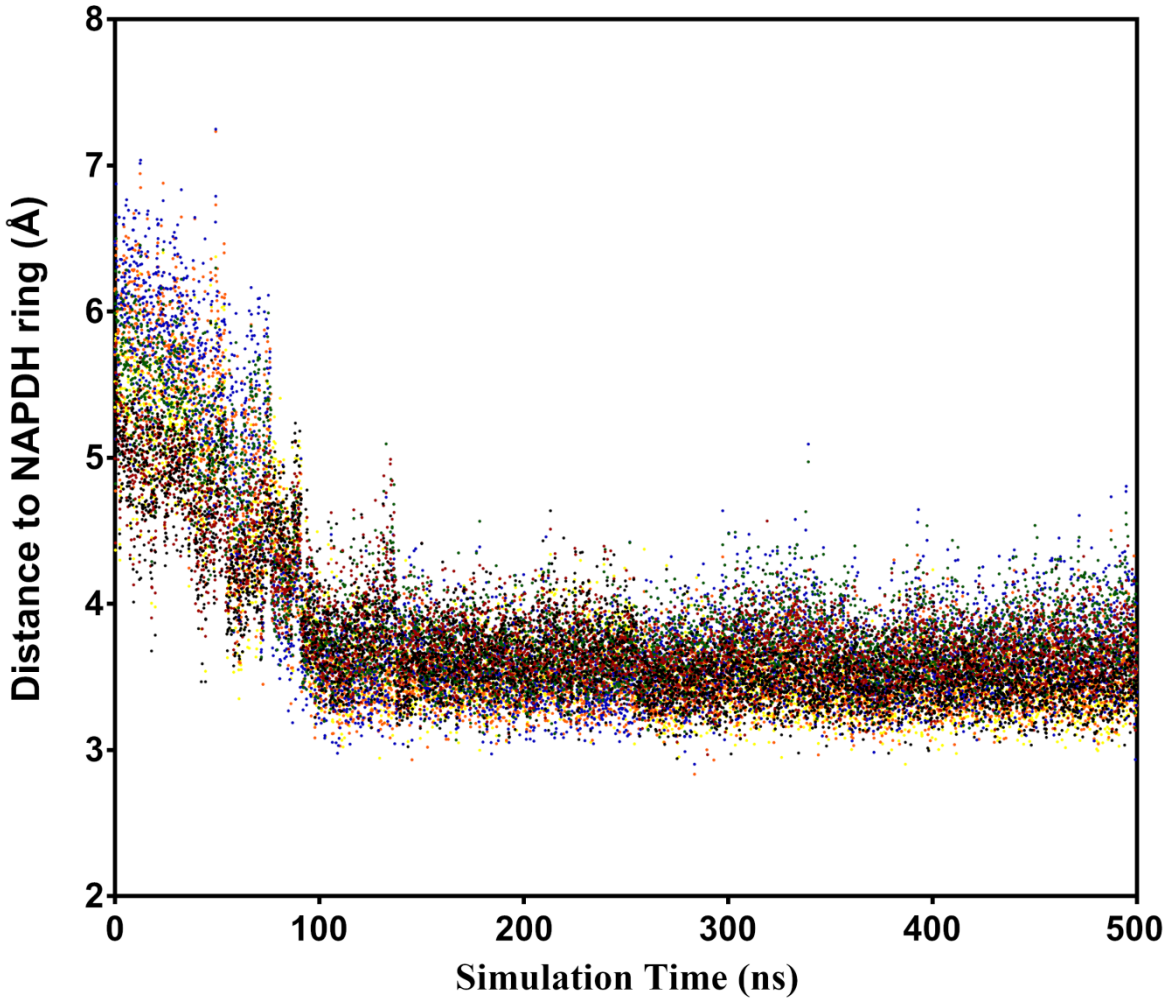

Figure S4. Distance between the atoms of the tranilast and NADPH rings to visualise stacking interactions in the 500 ns simulation. The distances between the tranilast-NADPH aromatic ring atoms C3-C5N (black), C4-C6N (red), C6-N1N (green), C7-C2N (blue), C8-C3N (orange) and C9-C4N (yellow) are shown as colored dots.

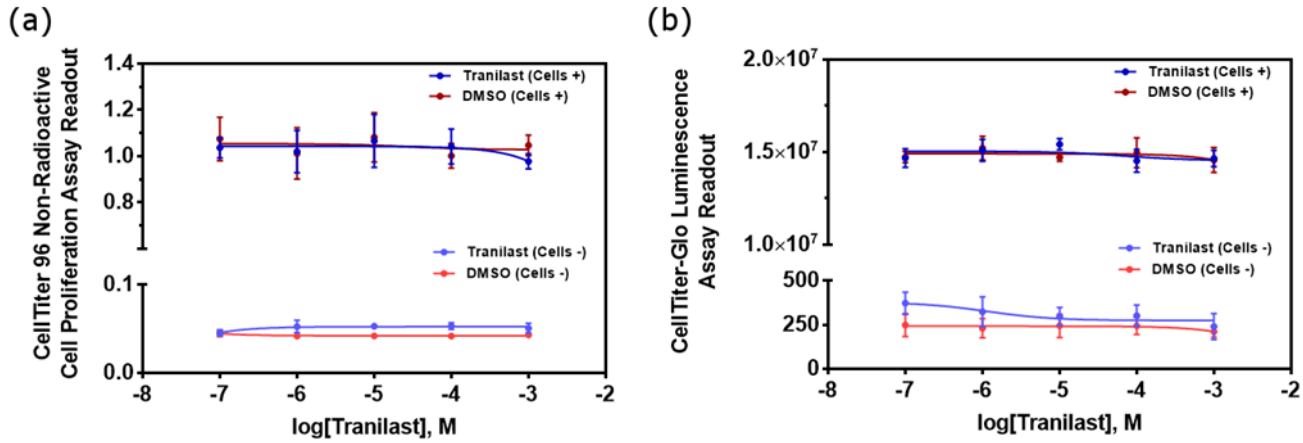

Figure S5. Effect of tranilast on cell viability and metabolism. a) The 570 nm absorbance readout in SH-SY5Y cells of coloured formazan product after treatment with a dose range of tranilast, quantified using the CellTiter® 96 Non-Radioactive Cell Proliferation Assay. b) Luminescence readout of SH-SY5Y intracellular ATP after treatment with a dose range of tranilast, quantified using the CellTiter-Glo® Luminescent Cell Viability Assay. All data is presented as mean ± SEM, n=3 for each assay point, including assay controls (DMSO and cell free wells).

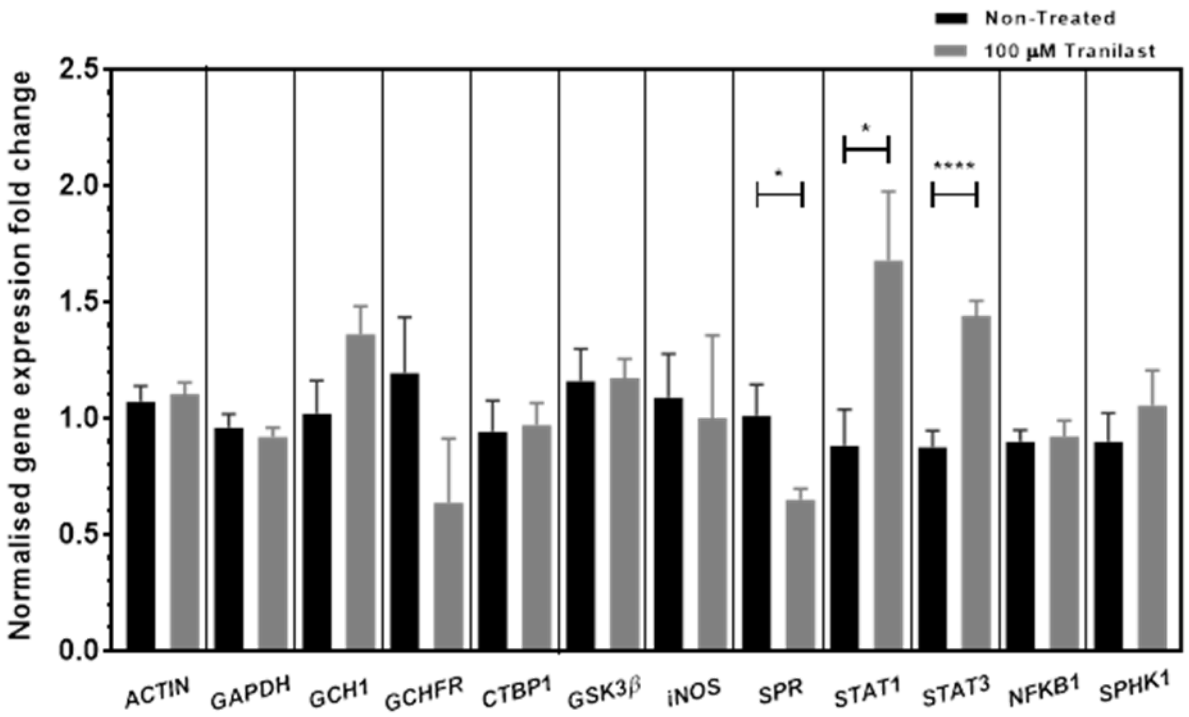

Figure S6. Expression changes measured by qRT-PCR of various genes of interest in the BH_4 pathway in RNA extracted from SH-SY5Y cells after 24 hour treatment with 100 µM tranilast. Data was normalised vs ACTIN and GAPDH. Results are presented as mean ± SEM (n=3). One-way ANOVA with Tukey's post-hoc test was performed (* = $p \leq 0.05$, **** = $p \leq 0.0001$).

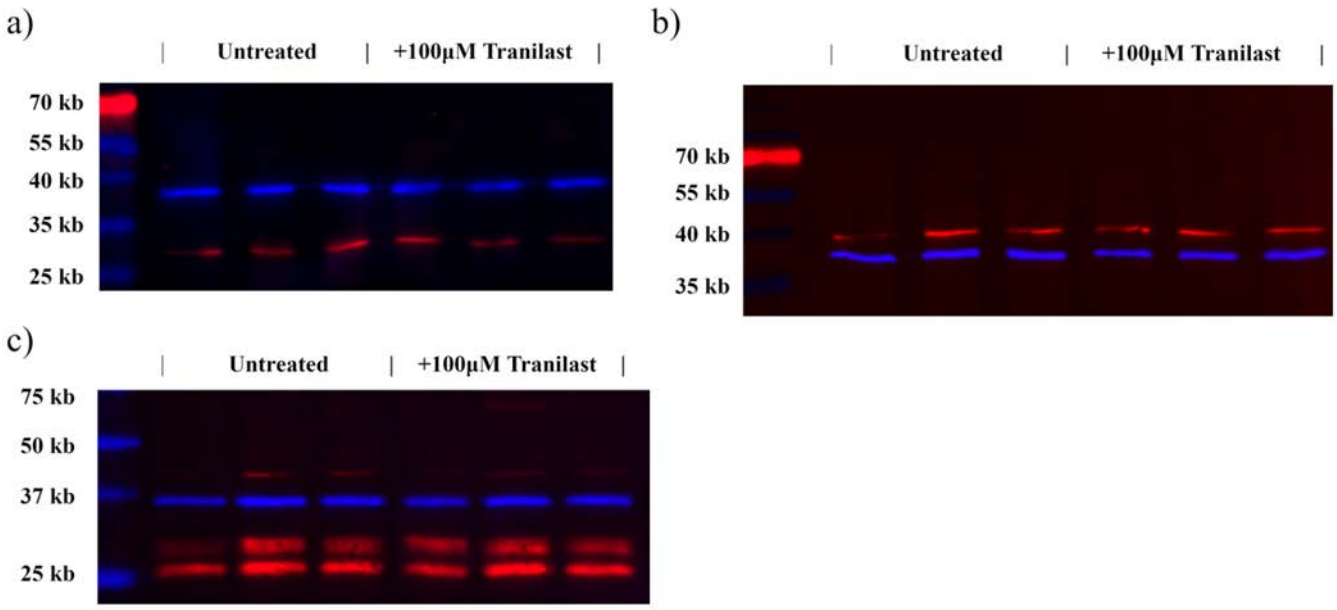

Figure S7. Western blot images of (a) SPR, (b) STAT3 and (c) GCH1. Three replicates of untreated and 100 µM tranilast treated protein extracts are shown in each gel. GAPDH (37 kb, blue band) was used as the loading control.

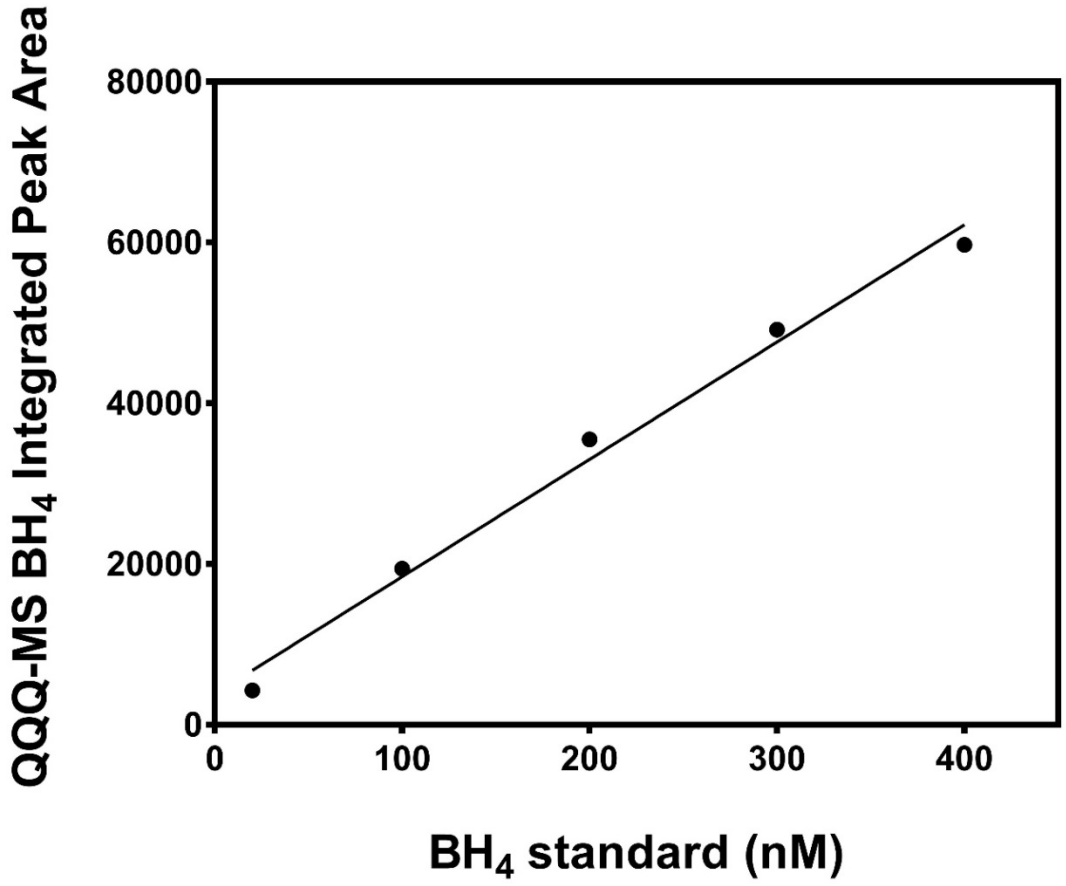

Figure S8. QQQ-MS quantification of the BH_4 standard for determining the limit of detection of the instrument and system parameters. The R^2 value for the linear regression curve was 0.989.